Advanced Powder Technology xxx (xxxx) xxx

Contents lists available at ScienceDirect

Advanced Powder Technology

journal homepage: www.elsevier.com/locate/apt

Original Research Paper

A facile synthesis of α-Ni(OH)$_2$-CNT composite films for supercapacitor application

S.B. Abitkar [a,b], P.R. Jadhav [c,d], N.L. Tarwal [c], A.V. Moholkar [b,1], C.E. Patil [a,*]

[a] Department of Physics, Dr. Patangrao Kadam Mahavidyalaya, Sangaliwadi, Sangali 416416, M.S., India
[b] Thin Film Nanomaterials Laboratory, Department of Physics, Shivaji University, Kolhapur 416004, M.S., India
[c] Thin Film Materials Laboratory, Department of Physics, Shivaji University, Kolhapur 416004, M.S., India
[d] Post Graduate Department of Physics, Devchand College, Arjunnagar 591269, M.S., India

ARTICLE INFO

Article history:
Received 30 November 2018
Received in revised form 8 July 2019
Accepted 10 July 2019
Available online xxxx

Keywords:
Supercapacitor
EIS
α-Ni(OH)$_2$-CNT composite films

ABSTRACT

The α-Ni(OH)$_2$-CNT composite films have been successfully synthesized by a simple chemical method and their supercapacitive properties were investigated by variation of CNT. The structural, compositional, morphological, wettability and electrochemical properties of the composite films were studied by using various characterization techniques. X-ray diffraction analysis revealed that the synthesized composite films are polycrystalline in nature. FT-Raman spectroscopy result showed the characteristic Raman band of CNT and α-Ni(OH)$_2$ which confirmed the formation of α-Ni(OH)$_2$-CNT composite. SEM micrographs showed porous microstructure of the synthesized films and hydrophilic nature of the films was confirmed from wettability studies. Furthermore, the effect of the variation of CNT on the electrochemical properties of the synthesized composite films was discussed. The electrochemical performance of the composite films was studied by using cyclic voltammetry (CV) and Galvanostatic charge–discharge (GCD) techniques. The α-Ni(OH)$_2$-CNT composite showed highest specific capacitance of 544 F g^{-1} with high retention capability of 85% after 1500th cycle and excellent cycling stability.

1. Introduction

Electrochemical supercapacitor has raised a great attention for high power energy storage applications because of their excellent cycling strength and high power density [1,2]. Also, it store energy in the form of electric charges which are environmentally friendly. Depending upon the charge storage mechanism, supercapacitor can be divided into two type's viz electrochemical double layer capacitor (EDLC) and pseudocapacitor [1,3]. However, pseudocapacitor has been extensively focused as compared to EDLC owing to their high specific capacitance [2]. The various pseudocapacitive materials, such as transition metal oxides/hydroxides like RuO_2, MnO_2, NiO, Ni(OH)$_2$, and Co(OH)$_2$ has been successfully used as electrode materials for supercapacitor applications [4–8]. Among these materials, Ni(OH)$_2$ has been widely studied for supercapacitor applications by reason of its high theoretical specific capacitance, relatively good chemical stability and environmentally friendly nature [9]. But still have limitations in practical applications because of its low energy density (ED) and low electrical conductivity. By considering these limitations, the development of new advanced composite electrode material for supercapacitor applications is a need of an hour. Recently, carbon based materials are extensively used for electrochemical capacitor applications to enhance their supercapacitive performance. It ranges from activated carbon (AC) to carbon nanotube (CNT) [10–12]. Especially, CNT has been found to be an excellent form of carbon over the other carbonaceous materials and have attracted an extensive attention to prepare composite with metal oxides/hydroxides for supercapacitor electrodes because of its high electrochemically accessible surface area, excellent chemical stability and low resistivity [13,14]. Additionally, CNT is used to alter the physical properties of metal oxides that are used for various applications such as solar cells [15], electrochromism [16], electrochemical sensors [10] and supercapacitors [17], respectively.

M. Kazazi et al. [18] have prepared nanoflakes nickel oxide-carbon nanotube (NiO-CNT) composite thin films by electrophoretic deposition for high-performance pseudocapacitor applications. They have reported that the prepared NiO-CNT composite electrode exhibited excellent pseudocapacitive behavior

* Corresponding author.
E-mail addresses: avmoholkar@gmail.com (A.V. Moholkar), cepatil4618@yahoo.co.in (C.E. Patil).
[1] Co-corresponding author.

https://doi.org/10.1016/j.apt.2019.07.008
0921-8831/

with a high specific capacitance of 786 F g^{-1} and 89.8% of capacitance retention after 1000th cycles as compared to pure NiO electrode. They have concluded that the uniformly dispersed CNT in the electrode that can provide fast and easy conductive pathway for transport of electrons into the active area of electrode material. Cheng et al. [17] have facile synthesized $Ni(OH)_2$/CNTs nanoflake composites, which showed improved performance for supercapacitor applications and gives a specific capacitance of 720 F g^{-1}. They have reported the better progress in electrochemical performance due to the synergetic effect of hydroxides and CNTs. Dai et al. [19] have synthesized CNT-NiO nanocomposite by chemical conversion route and exhibited the high specific capacitance of 759 F g^{-1} in 6 M KOH electrolyte due to the synergistic effects.

In the present manuscript, a simple chemical bath deposition (CBD) technique is used for the preparation of nickel hydroxide powder. After that an easy and cost-effective doctor blade method is used for the synthesis of α-$Ni(OH)_2$-CNT composite films and their supercapacitive properties have reported. Such an easily synthesized electrode gives the high specific capacitance with remarkable rate ability and excellent cycling strength in 1 M KOH electrolyte. Also, the effect of CNT variation on the electrochemical properties of the as-prepared α-$Ni(OH)_2$-CNT composite films is studied systematically and reported.

2. Experimental details

2.1. Synthesis of α-$Ni(OH)_2$-CNT composite films

The chemicals were of analytical grade (AR) used without further purification. Multi-walled carbon nanotube (MWCNT) was purchased from Monad Nanotech Pvt. Ltd., Mumbai, and used without further purification. For preparation of the precursor solution, double-distilled water (DDW) was used. Scheme 1 represents the steps involved for the synthesis of flower like microstructure α-$Ni(OH)_2$-CNT composite film. Initially, the nickel hydroxide powder was prepared by using chemical bath deposition (CBD) method. In this process, nickel sulfate ($NiSO_4{\cdot}6H_2O$) as a nickel precursor, potassium persulfate ($K_2S_2O_8$) as an oxidizing agent and aqueous ammonia as a complexing agent were used. In particular, 20 ml nickel sulfate (0.6 M) solution and 15 ml potassium persulfate (0.25 M) solution were mixed in a 100 ml beaker and stirred well at room temperature till its absolute dissolution and then get green colored solution. Further, aqueous ammonia was added slowly into the stirring solution to get pH 10.8 of the solution. Afterward, the brown color precipitating solution was formed in a 100 ml beaker. This obtained precipitate was filtered by using Whatman filter paper and again washed several times with double distilled water to remove the unwanted impurities. Finally, this washed precipitate was dried for 24 h at room temperature. Following this procedure the brown color nickel hydroxide powder was collected.

Further, the mixture of 0.5 g as-synthesized nickel hydroxide powder, 0.05 g polyvinilidene fluoride, 0.025 g CNT and a small amount of N-methyl-2-pyrrolidone was ground in agate mortar till the paste was formed. This paste was deposited on stainless steel substrate by doctor blade method followed by annealing at 300 °C for 1 h in an ambient atmosphere to remove the binders. The resulting product α-$Ni(OH)_2$-CNT was denoted as composite film NC-1. The above procedure was repeated by addition of 0.05 g, 0.075 g and 0.1 g CNT and these synthesized films were denoted as composite films NC-2, NC-3 and NC-4, respectively.

2.2. Materials characterization

The identification of phase and crystalline structure of composite films were characterized by D2 PHASER, Bruker, X-ray diffractometer with Cu-K_α radiation (λ = 1.5406 Å) over 10°-90°. FT-

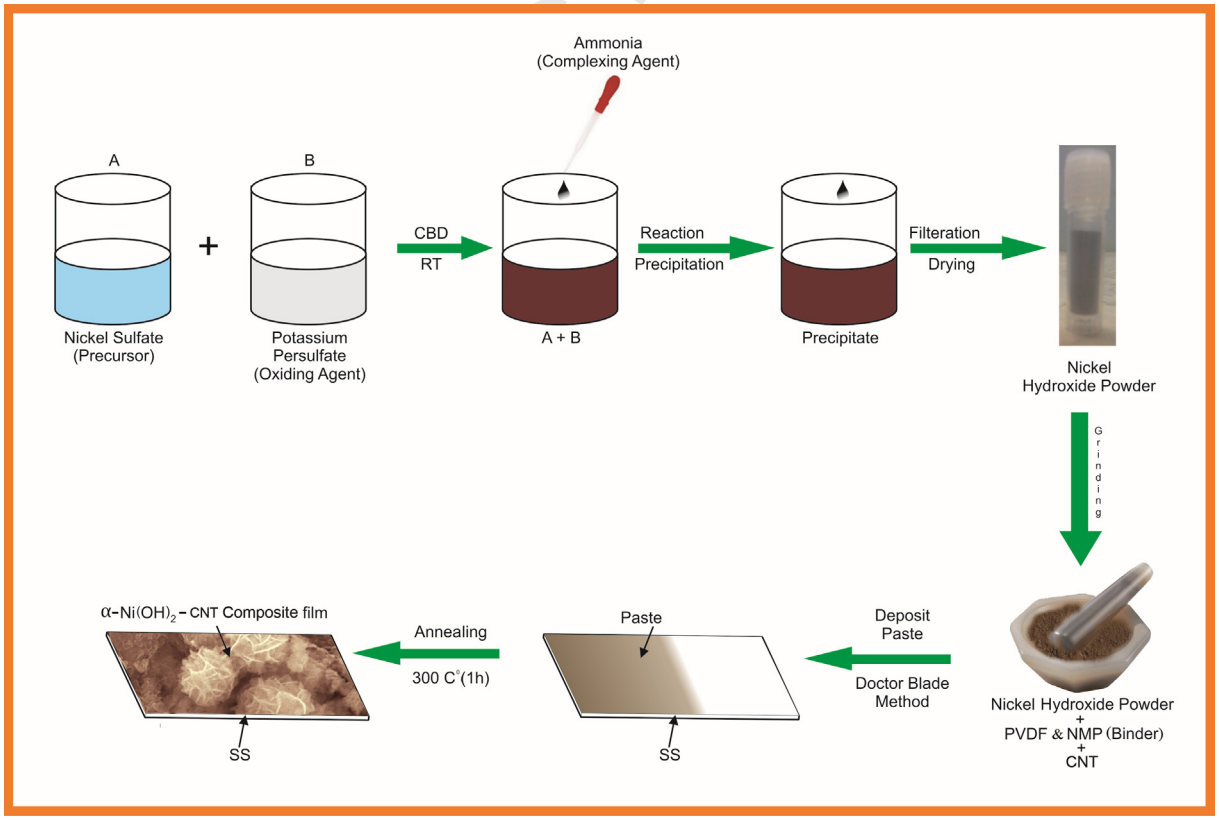

Scheme 1. Schematic of the steps involved for the synthesis of flowerlike porous microstructure α-$Ni(OH)_2$-CNT composite film.

Please cite this article as: S. B. Abitkar, P. R. Jadhav, N. L. Tarwal et al., A facile synthesis of α-$Ni(OH)_2$-CNT composite films for supercapacitor application, Advanced Powder Technology, https://doi.org/10.1016/j.apt.2019.07.008

Raman spectrum was recorded by using Bruker Multi RAM, Germany over 200–2000 cm^{-1} excited with the Argon 488 nm laser source obtained at room temperature. Surface morphological analysis of the synthesized composite films was carried out by using JEOL JSM-6360 Japan made scanning electron microscopy (SEM). The identification of the elements onto the surface of composite film was analyzed by energy dispersive X-ray analysis (EDX) connected with FE-SEM instrument (FE-SEM, TESCAN). Wettability analysis of the composite films was studied by using Holmarc's contact angle meter (model no: HO-IAD-CAM-01). Electrochemical measurements (Cyclic Voltammetry, galvonostatic charge discharge and electrochemical impedance spectroscopy analysis) were carried out in 1 M KOH electrolyte by using Metrohm's Autolab 320 N with three-electrode cell method, wherein graphite and the saturated calomel electrode (SCE) were used as a counter and the reference electrode, respectively. The composite film α-Ni $(OH)_2$-CNT was prepared by doctor blade method and used as working electrode.

3. Results and discussion

3.1. XRD studies

Fig. 1(a–d) shows the XRD patterns of NC-1, NC-2, NC-3 and NC-4 composite films respectively. It clearly shows that all the films are polycrystalline in nature. The diffraction peaks are located at 12.2°, 33.5°, and 59.6°, along the (0 0 3), (1 0 1) and (1 1 0) planes respectively, which clearly corroborates the structure of pure α-$Ni(OH)_2$ phase [18]. Furthermore, the observed and calculated 'd' values of diffraction peaks for α-$Ni(OH)_2$ are matched well with standard JCPDS card no. 38-0715. Also, it is seen that, there is a predominant diffraction peak located at 26.1° along the (0 0 2) plane, which confirms the formation of CNT. The corresponding 'd' value of diffraction peak for CNT is matched well with standard JCPDS card No. 75-1621 with hexagonal phase [18,20]. The above XRD results clearly confirms the formation of α-$Ni(OH)_2$-CNT composite. Also, in XRD pattern the stainless steel peaks are observed at 43.14°, 44.07°, 50.27° and 74.20°, respectively which are indexed by symbol *. The crystallite size of the composite films is calculated by using the Scherrer's relation [21].

$$D = \frac{0.9\lambda}{\beta \cos \theta} \quad (1)$$

where D is the crystallite size in nm, λ is an incident X-ray wavelength of Cu K_α line, β is the full-width half-maximum (FWHM) of the diffraction peak and θ is the Bragg's diffraction angle in degree. The calculated value of crystallite size for all the composite films is found to be in the range of 30–36 nm. Jahromi et al reported that the influence of nickel oxide nanoparticles on the supercapacitive performance [22].

3.2. Raman spectroscopic analysis

The Raman spectrum of NC-4 composite film is shown in Fig. 2. Three distinct peaks are observed at 503, 1331 and 1586 cm^{-1}. Raman peak at 503 cm^{-1} corresponds to vibrational lattice mode of Ni-OH and confirms the formation of α-$Ni(OH)_2$ [20]. The two bands at 1331 cm^{-1} (D band) and 1586 cm^{-1} (G band) reveal the typical CNT bands [23,24]. Raman band at 1586 cm^{-1} originates from Raman active in-plane atomic displacement E_{2g} mode [23]. The Raman profile shows the formation of α-$Ni(OH)_2$-CNT composite film without impurities. The results analyzed from Raman analysis are well consistent with XRD analysis.

3.3. Morphological studies and energy dispersive X-ray (EDX) analysis

Fig. 3(a–d) represents the SEM micrographs of all synthesized α-$Ni(OH)_2$-CNT composite films such as NC-1, NC-2, NC-3 and NC-4, respectively. In synthesis process, the mixture of $Ni(OH)_2$ and CNT was ground in agate mortar to form strong adhesion between them and also the quantity of $Ni(OH)_2$ was more than that of CNT in the composite. Consequently the CNT merged into the $Ni(OH)_2$ surface and formed together as flower-like porous microstructures as seen in Fig. 3 (b-d), suggesting that the structural interaction as well as porosity of the composite film is preserved well after addition of CNT [25,26]. Moreover it is seen that, these microstructures are getting agglomerated well because of strong interactions between $Ni(OH)_2$ and CNT due to grinding, and formed the abundant hollow spacing in the composite, which is increased gradually with addition of CNT [25,27]. This unique morphological surface provides more electrochemically active sites to increase the interfacial contact area between electrode surface and electrolyte for an easy ionic transportation during charging-discharging processes, and consequently enhances the electro-

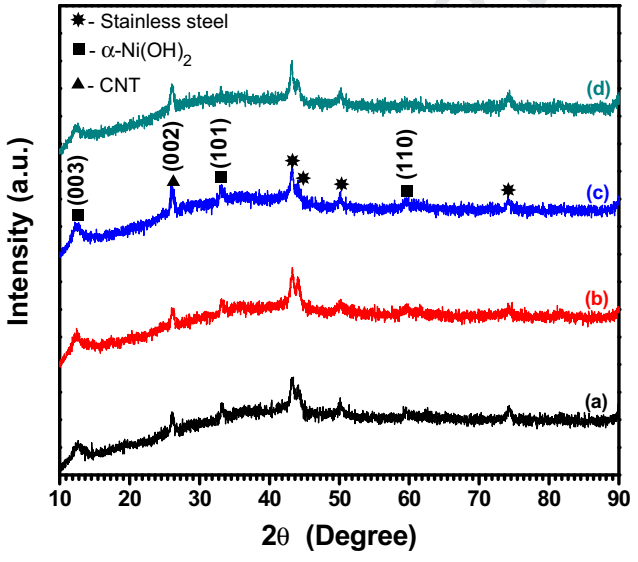

Fig. 1. X-ray diffraction patterns of $Ni(OH)_2$-CNT composite films: (a) NC-1, (b) NC-2, (c) NC-3 and (d) NC-4.

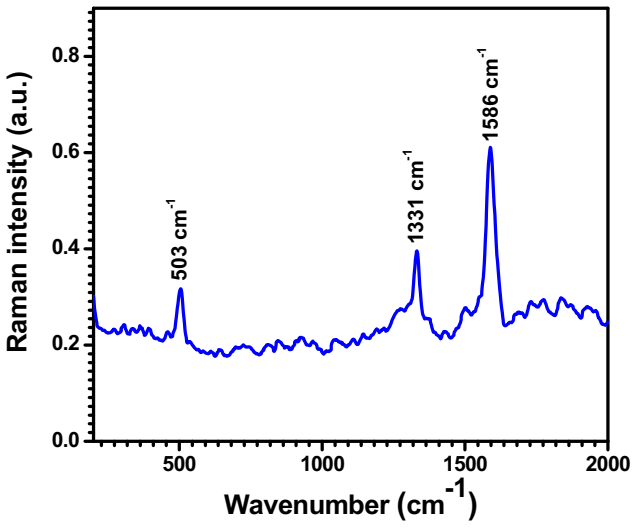

Fig. 2. Raman spectrum of α-$Ni(OH)_2$-CNT composite film (NC-4 composite film).

Please cite this article as: S. B. Abitkar, P. R. Jadhav, N. L. Tarwal et al., A facile synthesis of α-$Ni(OH)_2$-CNT composite films for supercapacitor application, Advanced Powder Technology, https://doi.org/10.1016/j.apt.2019.07.008

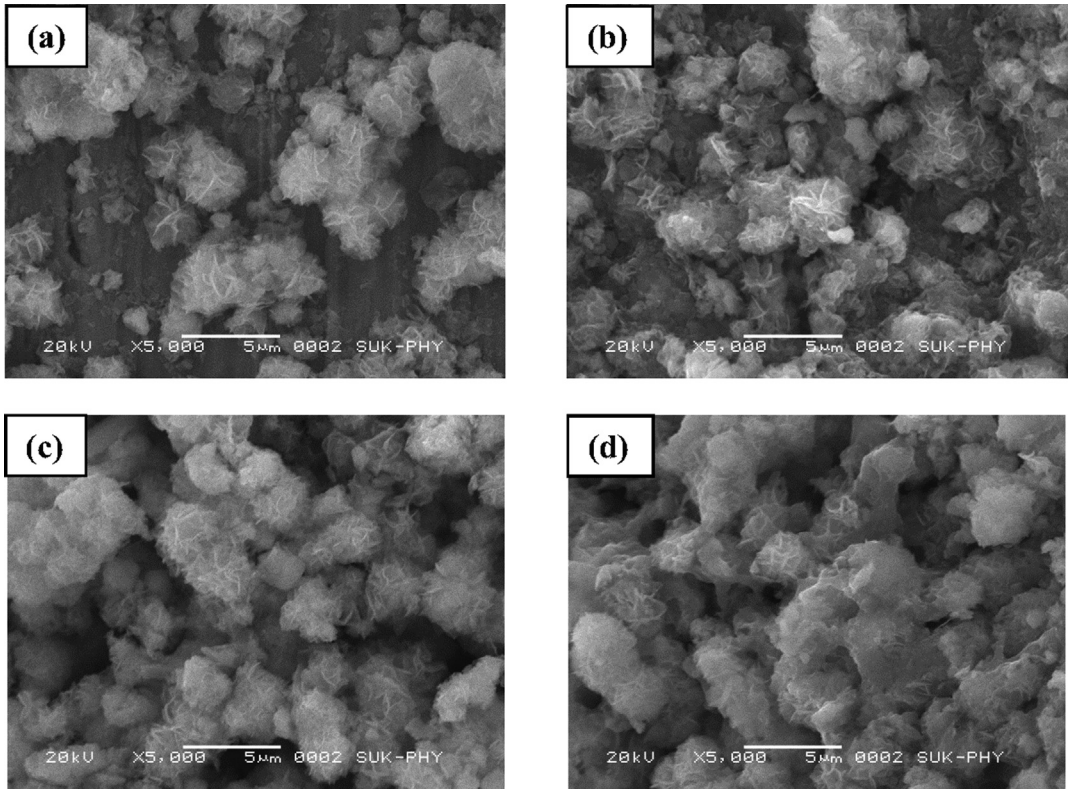

Fig. 3. SEM images of α-$Ni(OH)_2$-CNT composite films: (a) NC-1, (b) NC-2, (c) NC-3 and (d) NC-4.

chemical properties of the material, which is beneficial for supercapacitor application [18]. Fig. 4 illustrates that the typical EDX spectrum of the synthesized composite film NC-4. The prominent peaks of Ni, O and C elements are clearly visible in EDX spectrum which confirms the synthesized film is composite of $Ni(OH)_2$ and CNT. The compositional values in atomic percentage of Ni, O and C elements are observed as 14.73, 53.71 and 31.56, respectively.

3.4. Wettability studies

Wettability analysis of the composite film is empirically evaluated by the measurement of contact angle (θ) between water droplet and the surface of the film. The water contact angle value is directly related to the chemical composition, presence of local inhomogeneity's and geometrical surface of the films. A water contact angle (θ) should be less than 90° consisting of hydrophilic surface of the material. Fig. 5(a–d) represents the water contact angle images of all synthesized composite films NC-1, NC-2, NC-3 and NC-4 respectively. The measured contact angle values of all the films indicate hydrophilic surface which is more important parameter for good performance of electrode material. The SEM micrograph of all composite films shows the presence of abundant hollow spacing around the porous microstructures. A water droplet placed on this unique surface is absorbed by these hollow spacing and porous microstructures and then improve the hydrophilic surface of the composite. Also, the hydroxide group present in the α-$Ni(OH)_2$-CNT composite may help the absorption of ions to improve the hydrophilicity of the CNT [2]. So the contact angle of water drop on α-$Ni(OH)_2$-CNT composite film decreases with addition of CNT. Shaikh et al. [28] reported that the surface of CPCNT films transform from hydrophobic to hydrophilic (120 to 65°) with annealing temperature. Yu et al. [29] reported that the contact angle of 16.3° was obtained with the 7 wt% of CNT content. Ouyang et al. [30] reported that the Ni-Ag/SWCNTs/GCE composite electrode exhibited the best hydrophilicity due to the smallest contact angle of 30.8°. In the present case, the composite film NC-4 gives lower contact angle value of 57° containing superior hydrophilic surface, which provides the high effective surface area that can improve conductivity of the material by reducing the effective resistances during ionic exchanging process at electrode-electrolyte interface. The hydrophilic behavior of the film permits an easier access for redox reactions which is beneficial for supercapacitor applications. Also, such an important parameter plays an effective role for reducing diffusion path length of the ions during charge-discharge processes [31].

3.5. Cyclic voltammetry (CV) studies

By CV and GCD measurements the capacitive nature of the material can be examined. Fig. 6(a–d) shows the cyclic voltammograms (CV) curves of all α-$Ni(OH)_2$-CNT composite films i.e. NC-1, NC-2, NC-3 and NC-4, respectively at different scan rates from 10 to 100 mVs^{-1}. The CV curves were recorded in the potential window of −1.0 V to 0.4 V vs SCE in 1 M KOH electrolyte. It is seen that, the recorded CV curves of all composite films are nearly identical and exhibit a quasi rectangular shape with an oxidation and reduction peaks respectively, which implies an ideal pseudocapacitive characteristic of the material [32]. Also, the charge-discharge processes of the films are associated with an oxidation and reduction pair. The corresponding faradaic redox reaction in which anodic peak at 0.3 V vs SCE correspond to the oxidation of α-$Ni(OH)_2$ to γ-NiOOH, whereas the cathodic peak at −0.5 V vs SCE correspond to the reverse process is given as follows [32]:

$$\alpha\text{-}Ni(OH)_2 + OH^- = \gamma\text{-}NiOOH + H_2O + e^- \quad (2)$$

From Fig. 6(a–d) it is seen that, the area under the CV curve increases with increasing the scan rate from 10 to 100 mVs^{-1} which reveals that the voltammetric current is directly proportional to the

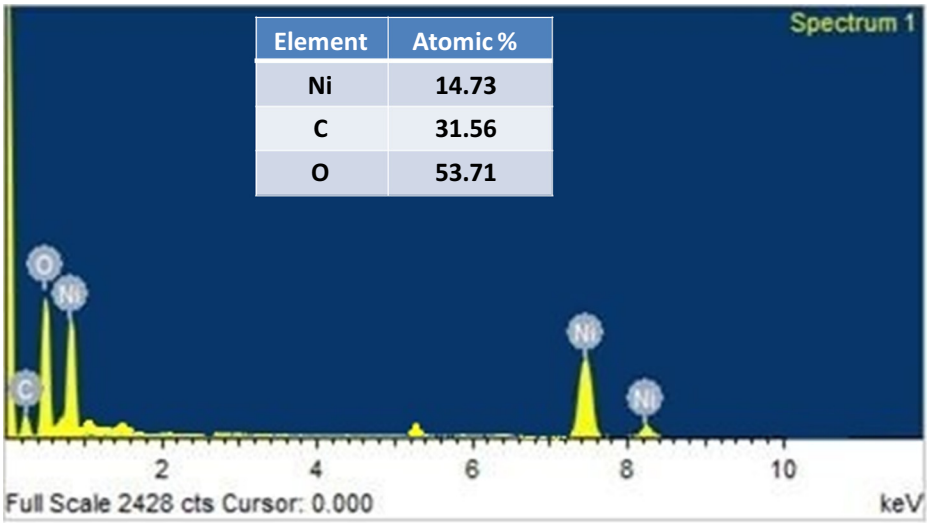

Fig. 4. EDX spectrum of typical α-Ni(OH)$_2$-CNT composite film (NC-4 composite film).

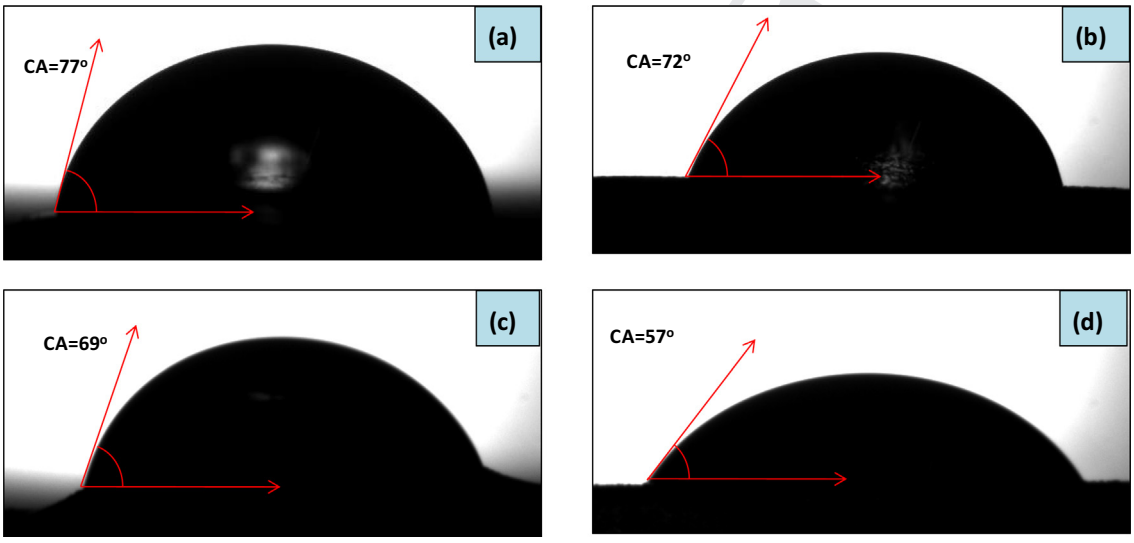

Fig. 5. Water contact angle images of α-Ni(OH)$_2$-CNT composite films: (a) NC-1, (b) NC-2, (c) NC-3 and (d) NC-4.

scan rate [33]. Moreover, the current density of both anodic and cathodic peaks smoothly increases by increasing the scan rate but, there is no any apparent changes in the shape of the CV curves which, signify lowest contact resistance of the electrode for better electrochemical processes [34]. Nevertheless, the specific capacitance of the composite film decreases with increasing the scan rate because of moderated reaction mechanism between electrode-electrolyte interfaces. Fig. 7 shows the collectively depicted CV curve of all synthesized composite films NC-1, NC-2, NC-3 and NC-4, respectively measured at a constant scan rate of 10 mVs^{-1} in 1 M KOH electrolyte. It indicates that an area under the CV curve of the composite films increases with increasing the quantity of the CNT. The CV curve area is used to calculate the specific capacitance of the composite film by using the following equation [35], and presented in Table 1.

$$C_s = \frac{\int i\,dv}{2(m)(\Delta V)(Vs)} \quad (3)$$

where C_s is the specific capacitance, ∫ i dv is the area of the CV curves within the assigned potential range, m is the mass of the active material on a substrate, ΔV is the potential window, and Vs is the scan rate. It is seen that the composite film NC-4 acquire highest area under the CV curve which provides the highest specific capacitance of 544 F g^{-1} as compared to other composite films. Hence, it corroborates, the role of CNT is important to increase the specific capacitance of the composite film. The NC-4 sample exhibits lowest water contact angle and maximum surface area which offer the large number of electrochemical active sites for the intercalation of ions from the electrolyte to the surface of the electrode and hence faster diffusion into the active electrode material takes place.

3.6. Galvanostatic charge-discharge (GCD) studies

The GCD study is very important for resolving the charge-discharge stability, energy density and power density of the material. Fig. 8(a–d) shows the charge-discharge curves of all α-Ni(OH)$_2$-CNT composite films i.e. NC-1, NC-2, NC-3 and NC-4, respectively at constant current density of 1 mA/cm^2 were recorded in the potential window of −1.0 V to 0.4 V vs SCE in 1 M KOH electrolyte. All the GCD curves are seen as non-triangular in shape which confirms the faradaic (pseudocapacitive) behavior of the

Please cite this article as: S. B. Abitkar, P. R. Jadhav, N. L. Tarwal et al., A facile synthesis of α-Ni(OH)$_2$-CNT composite films for supercapacitor application, Advanced Powder Technology, https://doi.org/10.1016/j.apt.2019.07.008

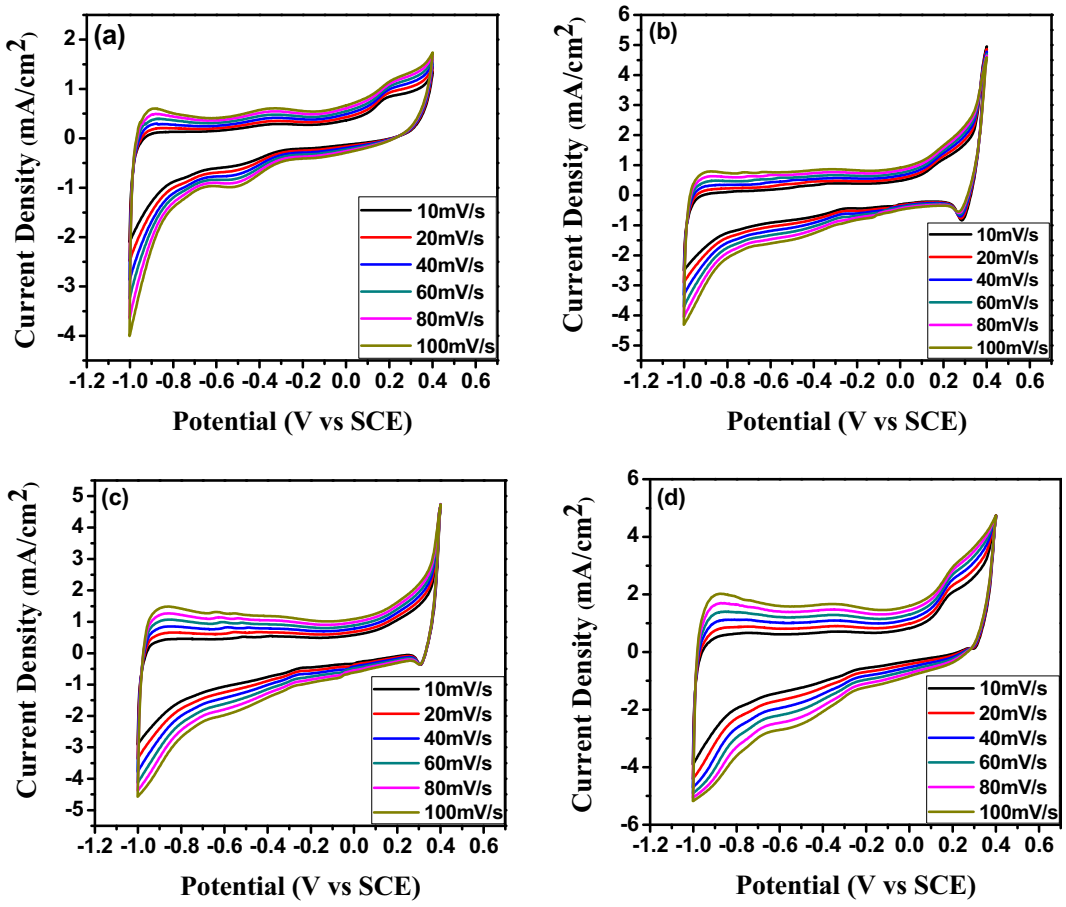

Fig. 6. Cyclic voltammograms of α-$Ni(OH)_2$-CNT composite films: (a) NC-1, (b) NC-2, (c) NC-3 and (d) NC-4 in 1 M KOH electrolyte at various scan rates.

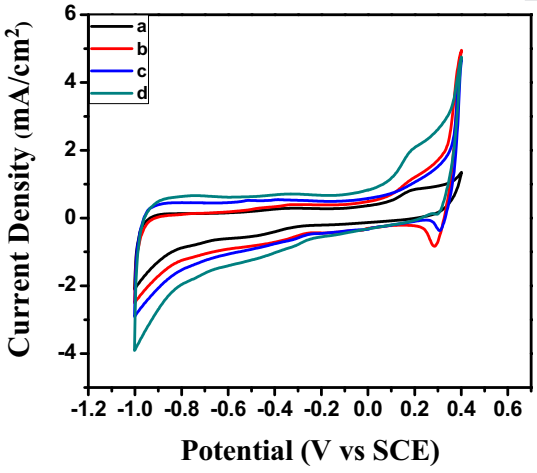

Fig. 7. Cyclic voltammograms of α-$Ni(OH)_2$-CNT composite films: (a) NC-1, (b) NC-2, (c) NC-3 and (d) NC-4 in 1 M KOH electrolyte at constant scan rate of 10 mV/s.

electrode material [36]. From the slope of GCD curves, it is seen that the composite film NC-4 shows a longer discharging time and gives maximum specific capacitance of 537 F g^{-1} at 1 mA/cm^2. The specific capacitance (C_s), energy density (E) and power density (P) of the composite films is calculated from discharge curves, according to the following equation [37],

$$C_s = \frac{I}{m(\Delta V/\Delta t)} \quad (4)$$

$$E = \frac{1}{2}C(\Delta V)^2 \quad (5)$$

$$P = \frac{E}{\Delta t} \quad (6)$$

where, I – applied current, m – mass of the deposited material onto the electrode, ΔV – discharge voltage range and Δt – discharge time. The calculated values of specific capacitance, energy density and power density of composite films are presented in Table 1. From Table 1 it clear that, the specific capacitance of α-$Ni(OH)_2$-

Table 1
Electrochemical performance evaluated for α-$Ni(OH)_2$-CNT composite films.

Sample code	Sp. capacitance by CV (F/g)	Sp. capacitance by CD (F/g)	Energy density (Wh/kg)	Power density (kW/kg)	R_{ct} (Ω)
NC-1	380	364	13.48	3.10	9.20
NC-2	421	427	15.71	3.67	7.80
NC-3	472	480	17.82	3.90	6.62
NC-4	544	537	21.25	4.78	3.32

Please cite this article as: S. B. Abitkar, P. R. Jadhav, N. L. Tarwal et al., A facile synthesis of α-$Ni(OH)_2$-CNT composite films for supercapacitor application, Advanced Powder Technology, https://doi.org/10.1016/j.apt.2019.07.008

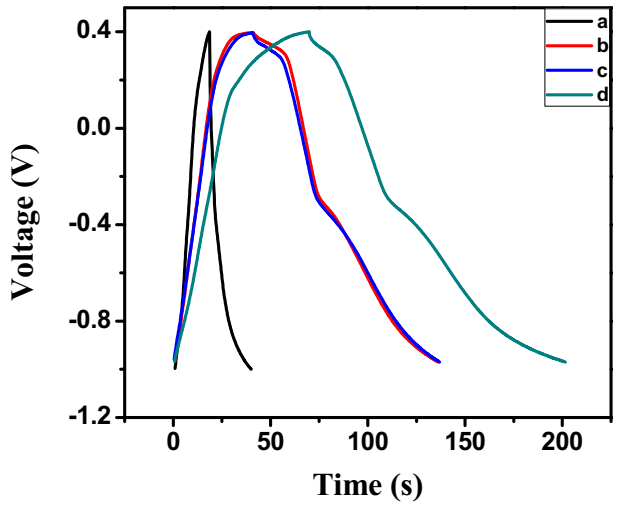

Fig. 8. Galvanostatic charge discharge curves of α-Ni(OH)$_2$-CNT composite films: (a) NC-1, (b) NC-2, (c) NC-3 and (d) NC-4 in 1 M KOH electrolyte at constant current density of 1 mA/cm^2.

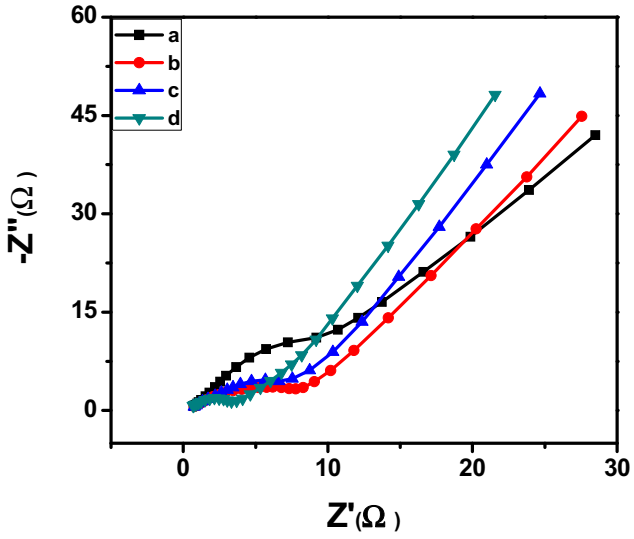

Fig. 10. Nyquist plot of α-Ni(OH)$_2$-CNT composite films: (a) NC-1, (b) NC-2, (c) NC-3 and (d) NC-4 in 1 M KOH electrolyte.

CNT composite films are improved due to the contribution of conductive nature of CNT, which provides higher accessible active sites for fast redox process. The stability test measurement is carried out for optimized NC-4 composite film in 1 M KOH electrolyte and the recorded curves are shown in Fig. 9. It is seen that the capacitive retention varies with the cycle number. The 85% capacitance retention is observed after 1500th cycle for typical composite film NC-4. The stability test indicates that, the composite film α-Ni(OH)$_2$-CNT attains good cycling capacity in 1 M KOH electrolyte and hence it is a powerful electrode material for electrochemical mechanism. Also, from Fig. 9 it is seen that, only 13% capacitive loss is occurred in an initial capacitance after 1000th cycle which reveal the remarkable rate capacity of α-Ni(OH)$_2$-CNT composite electrode.

3.7. Electrochemical impedance spectroscopy (EIS) studies

The EIS studies are being performed to understand the reaction kinetics of the material and to evaluate their overall resistance components. In EIS analysis the larger diameter semicircle observed in the high frequency region is related to the higher charge transfer resistance (R_{ct}) of the electrode-electrolyte interface and an inclined straight line behavior observed in the low frequency region which corresponds to the limiting ion diffusion process [38]. Fig. 10(a–d) shows the Nyquist plot of α-Ni(OH)$_2$-CNT composite films NC-1, NC-2, NC-3 and NC-4, respectively in the frequency range from 10 mHz to 1 MHz for 1 M KOH electrolyte. The EIS analysis exhibited that, the decrement in R_{ct} value of composite films which are given in Table 1. It indicates that the improvement in conductivity of the electrodes due to the addition of CNT in the composite [26]. It is observed that, the composite film NC-4 exhibits smaller semicircle provides lowest charge transfer resistance of the electrode-electrolyte interface and the higher slope offer the minimum ion diffusion resistance. Thus, the composite film NC-4 gives a very low R_{ct} value 3.32 Ω implying its high conductivity and high capacitance as compared to the other composite films [34,39].

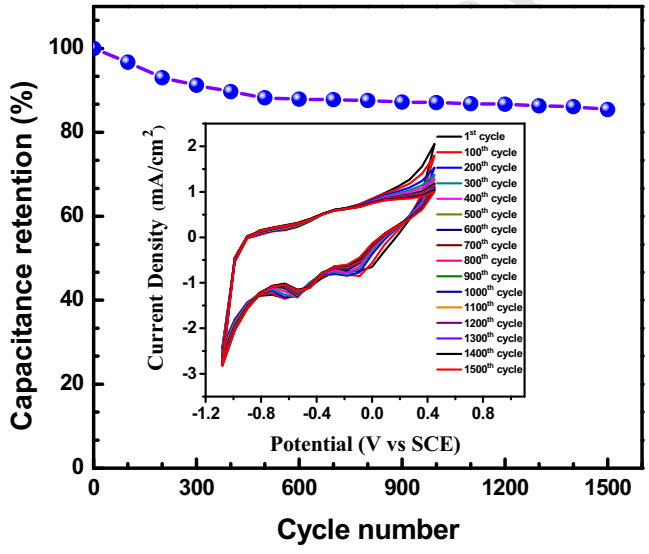

Fig. 9. Variation of specific capacitance (%) with respect to cycle numbers for α-Ni(OH)$_2$-CNT composite film (NC-4 composite film) in 1 M KOH electrolyte at a scan rate of 100 mV/s for 1500 cycles.

4. Conclusions

A flowerlike porous microstructure of α-Ni(OH)$_2$-CNT composite films have been synthesized by a simple and inexpensive doctor blade method. The composite films showed excellent supercapacitor properties in 1 M KOH electrolyte. X-ray diffraction analysis showed that the composite films are polycrystalline in nature. FT-Raman analysis confirms the well formation of α-Ni(OH)$_2$-CNT composite. Morphological studies shows porous microstructure of the synthesized films and the wettability studies shows superior hydrophilic surface of the composite film (NC-4). The electrochemical analysis showed that the α-Ni(OH)$_2$-CNT composite film (NC-4) gives highest specific capacitance of 544 F g^{-1} and higher retention capability of (85%) after 1500th cycle. Moreover, it exhibited the high energy density of 21.25 Wh/kg and high power density of 4.78 kW/kg. From EIS measurements it confirmed that the α-Ni(OH)$_2$-CNT composite electrode provides very lowest charge transfer resistance (3.32 Ω) of the electrode-electrolyte interface implying higher conductivity of the material. Thus, it is concluded that, the α-Ni(OH)$_2$-CNT composite film (NC-4) is more appropriate material for supercapacitor applications.

Please cite this article as: S. B. Abitkar, P. R. Jadhav, N. L. Tarwal et al., A facile synthesis of α-Ni(OH)$_2$-CNT composite films for supercapacitor application, Advanced Powder Technology, https://doi.org/10.1016/j.apt.2019.07.008

Acknowledgements

The authors gratefully acknowledge to Physics Instrumentation Facility Centre (PIFC), Department of Physics, Shivaji University Kolhapur for various characterization purposes. One of the author C. E. Patil wishes to acknowledge to UGC, New Delhi for financial support through F. No. 41-885/2012 (SR).

References

[1] B. Kim, S. Sy, A. Yu, J. Zhang, Electrochemical supercapacitors for energy storage and conversion, Handbook of Clean Energy Systems, John Wiley & Sons, Ltd., 2015.
[2] G. Wang, L. Zhang, J. Zhang, A review of electrode materials for electrochemical supercapacitors, Chem. Soc. Rev. 41 (2012) 797–828.
[3] X. Su, S. Li, S. Jiang, Z. Peng, X. Guan, X. Zheng, Superior capacitive behavior of porous activated carbon tubes derived from biomass waste-cotonier strobili fibers, Adv. Powder Technol. 29 (2018) 2097–2107.
[4] H. Cui, J. Xue, M. Wang, Synthesis of high electrochemical performance Ni $(OH)_2$ nanosheets through a solvent-free reaction for application in supercapacitor, Adv. Powder Technol. 26 (2015) 434–438.
[5] B.W. Chae, T. Amna, M.S. Hassan, S.S. Al-deyab, M. Khil, CeO_2-Cu_2O composite nanofibers: synthesis, characterization photocatalytic and electrochemical application, Adv. Powder Technol. 28 (2017) 230–235.
[6] W. Ma, Y. Feng, L. Wang, Y. Li, M. Shi, H. Cui, $Co_2(OH)_3Cl$ nanoparticles as new-type electrode material with high electrochemical performance for application in supercapacitor, Adv. Powder Technol. 28 (2017) 2642–2647.
[7] J.R. Zheng, B. Chen, W.K. Li, J.J. Zhu, L.P. Jiang, Electrochemical behavior of amorphous hydrous ruthenium oxide/active carbon composite electrodes for super-capacitor, Int. J. Mod. Phys. B 16 (2002) 4479–4483.
[8] P.R. Jadhav, M.P. Suryawanshi, D.S. Dalavi, D.S. Patil, E.A. Jo, S.S. Kolekar, A.A. Wali, M.M. Karanjkar, J.-H. Kim, P.S. Patil, Design and electro-synthesis of 3-D nanofibers of MnO_2 thin films and their application in high performance supercapacitor, Electrochim. Acta 176 (2015) 523–532.
[9] G.W. Yang, C.L. Xu, H.L. Li, Electrodeposited nickel hydroxide on nickel foam with ultrahigh capacitance, Chem. Commun. 48 (2008) 6537–6539.
[10] L. Zhao, J. Yu, S. Yue, L. Zhang, Z. Wang, P. Guo, Q. Liu, Nickel oxide/carbon nanotube nanocomposites prepared by atomic layer deposition for electrochemical sensing of hydroquinone and catechol, J. Electroanal. Chem. 808 (2018) 245–251.
[11] E. Frackowiak, Carbon materials for supercapacitor application, Phys. Chem. Chem. Phys. 9 (2007) 1774–1785.
[12] T. Chen, L. Dai, Carbon nanomaterials for high-performance supercapacitors, Mater. Today 16 (2013) 272–280.
[13] H. Pan, J. Li, Y.P. Feng, Carbon nanotubes for supercapacitor, Nanoscale Res. Lett. 5 (2010) 654–668.
[14] M.F.L. De Volder, S.H. Tawfick, R.H. Baughman, A.J. Hart, Carbon nanotubes: present and future commercial applications, Science 339 (2013) 535–539.
[15] S. Muduli, W. Lee, V. Dhas, S. Mujawar, M. Dubey, K. Vijayamohanan, S.H. Han, S. Ogale, Enhanced conversion efficiency in dye-sensitized solar cells based on hydrothermally synthesized TiO_2-MWCNT nanocomposites, Appl. Mater. Interfaces 1 (2009) 2030–2035.
[16] P.M. Kadam, N.L. Tarwal, S.S. Mali, H.P. Deshmukh, P.S. Patil, Enhanced electrochromic performance of f-MWCNT-WO_3 composite, Electrochim. Acta 58 (2011) 556–561.
[17] H. Cheng, A.D. Su, S. Li, S.T. Nguyen, L. Lu, C.Y.H. Lim, H.M. Duong, Facile synthesis and advanced performance of $Ni(OH)_2$/CNTs nanoflake composites on supercapacitor applications, Chem. Phys. Lett. 601 (2014) 168–173.
[18] M. Kazazi, Facile preparation of nanoflake-structured nickel oxide/carbon nanotube composite films by electrophoretic deposition as binder-free electrodes for high-performance pseudocapacitors, Curr. Appl. Phys. 17 (2017) 240–248.
[19] K. Dai, C. Liang, J. Dai, L. Lu, G. Zhu, Z. Liu, Q. Liu, Y. Zhang, High-yield synthesis of carbon nanotube-porous nickel oxide nanosheet hybrid and its electrochemical capacitance performance, Mater. Chem. Phys. 143 (2014) 1344–1351.
[20] S. Chen, J. Zhu, H. Zhou, X. Wang, One-step synthesis of low defect density carbon nanotube-doped $Ni(OH)_2$ nanosheets with improved electrochemical performances, RSC Adv. 1 (2011) 484–489.
[21] A.I. Inamdar, S.H. Mujawar, S.B. Sadale, A.C. Sonavane, M.B. Shelar, P.S. Shinde, P.S. Patil, Electrodeposited zinc oxide thin films: nucleation and growth mechanism, Sol. Energy Mater. Sol. Cells 91 (2007) 864–870.
[22] S. Pilban Jahromi, A. Pandikumar, B.T. Goh, Y.S. Lim, W.J. Basirun, H.N. Lim, N. M. Huang, Influence of particle size on performance of a nickel oxide nanoparticle-based supercapacitor, RSC Adv. 5 (2015) 14010–14019.
[23] X. Xie, L. Gao, Characterization of a manganese dioxide/carbon nanotube composite fabricated using an in situ coating method, Carbon 45 (2007) 2365–2373.
[24] H. Yi, H. Wang, Y. Jing, T. Peng, X. Wang, Asymmetric supercapacitors based on carbon nanotubes@NiO ultrathin nanosheets core-shell composites and MOF-derived porous carbon polyhedrons with super-long cycle life, J. Power Sources 285 (2015) 281–290.
[25] A.S. Adekunle, K.I. Ozoemena, Electrosynthesised metal (Ni, Fe, Co) oxide films on single-walled carbon nanotube platforms and their supercapacitance in acidic and neutral pH media, Electroanalysis 23 (2011) 971–979.
[26] Z.J. Yu, Y. Dai, W. Chen, Synthesis and characterization of $Ni(OH)_2$/multiwalled carbon nanotubes nanocomposites for electrochemical capacitors, Adv. Mater. Res. 239 (2011) 2968–2971.
[27] L. Li, Z.A. Hu, N. An, Y.Y. Yang, Z.M. Li, H.Y. Wu, Facile synthesis of MnO_2/CNTs composite for supercapacitor electrodes with long cycle stability, J. Phys. Chem. C 118 (2014) 22865–22872.
[28] J.S. Shaikh, R.C. Pawar, S.S. Mali, A.V. Moholkar, J.H. Kim, P.S. Patil, Effect of annealing on the supercapacitor performance of CuO-PAA/CNT films, J. Solid State Electrochem. 16 (2012) 25–33.
[29] W. Yu, H. Zhou, B.Q. Li, S. Ding, 3D printing of carbon nanotubes-based microsupercapacitors, Appl Mater Interfaces 9 (2017) 4597–4604.
[30] R. Ouyang, W. Li, Y. Yang, W. Zhang, K. Feng, T. Zong, Y. An, S. Zhou, Y. Miao, Morphology effect of Ni–Ag/Carbon nanomaterials on their electrocatalytic activity for glucose oxidation, Surf. Rev. Lett. 23 (2016) 1650059.
[31] S.T. Navale, V.V. Mali, S.A. Pawar, R.S. Mane, M. Naushad, F.J. Stadler, V.B. Patil, Electrochemical supercapacitor development based on electrodeposited nickel oxide film, RSC Adv. 5 (2015) 51961–51965.
[32] C.C. Lai, C.T. Lo, Effect of temperature on morphology and electrochemical capacitive properties of electrospun carbon nanofibers and nickel hydroxide composites, Electrochim. Acta. 174 (2015) 806–814.
[33] T.P. Gujar, V.R. Shinde, C.D. Lokhande, S.H. Han, Electrosynthesis of Bi_2O_3thin films and their use in electrochemical supercapacitors, J. Power Sources. 161 (2006) 1479–1485.
[34] P. Sun, H. Yi, T. Peng, Y. Jing, R. Wang, H. Wang, X. Wang, Ultrathin MnO_2 nanoflakes deposited on carbon nanotube networks for symmetrical supercapacitors with enhanced performance, J. Power Sources 341 (2017) 27–35.
[35] B.K. Kim, V. Chabot, A. Yu, Carbon nanomaterials supported $Ni(OH)_2$/NiO hybrid flower structure for supercapacitor, Electrochim. Acta. 109 (2013) 370–380.
[36] H. Gao, J. Xiang, Y. Cao, Hierarchically porous $CoFe_2O_4$ nanosheets supported on Ni foam with excellent electrochemical properties for asymmetric supercapacitors, Appl Surf Sci. 413 (2017) 351–359.
[37] A.L.M. Reddy, S. Ramaprabhu, Nanocrystalline metal oxides dispersed multiwalled carbon nanotubes as supercapacitor electrodes, J. Phys. Chem. C. 111 (2007) 7727–7734.
[38] L. Cao, M. Lu, H.L. Li, Preparation of mesoporous nanocrystalline Co_3O_4 and its applicability of porosity to the formation of electrochemical capacitance, J. Electrochem. Soc. 152 (2005) A871–A875.
[39] Y. Zheng, M. Zhang, P. Gao, Preparation and electrochemical properties of multiwalled carbon nanotubes-nickel oxide porous composite for supercapacitors, Mater. Res. Bull. 42 (2007) 1740–1747.

Please cite this article as: S. B. Abitkar, P. R. Jadhav, N. L. Tarwal et al., A facile synthesis of α-$Ni(OH)_2$-CNT composite films for supercapacitor application, Advanced Powder Technology, https://doi.org/10.1016/j.apt.2019.07.008